

1 **Novel genetic modules encoding high-level antibiotic-free protein**
2 **expression in probiotic lactobacilli**

3 Sourik Dey,^{1,†} Marc Blanch-Asensio,^{1,†} Sanjana Balaji Kuttae,¹ Shrikrishnan
4 Sankaran^{1*}

5 ¹ Bioprogrammable Materials, INM - Leibniz Institute for New Materials, Campus D2
6 2, 66123 Saarbrücken, Germany

7 *E-mail: Shrikrishnan.sankaran@leibniz-inm.de

8 † Authors contributed equally

9 **ABSTRACT**

10 Lactobacilli are ubiquitous in nature, often beneficially associated with animals as
11 commensals and probiotics, and are extensively used in food fermentation. Due to
12 this close-knit association, there is considerable interest to engineer them for
13 healthcare applications in both humans and animals, for which high-performance
14 and versatile genetic parts are greatly desired. For the first time, we describe two
15 genetic modules in *Lactiplantibacillus plantarum* that achieve high-level gene
16 expression using plasmids that can be retained without antibiotics, bacteriocins or
17 genomic manipulations. These include (i) a promoter, $P_{t\rho A}$, from a phylogenetically
18 distant bacterium, *Salmonella typhimurium*, that drives up to 5-fold higher level of
19 gene expression compared to previously reported promoters and (ii) multiple toxin-
20 antitoxin systems as a self-contained and easy-to-implement plasmid retention
21 strategy that facilitates the engineering of tunable transient Genetically Modified
22 Organisms. These modules and the fundamental factors underlying their

23 functionality that are described in this work will greatly contribute to expanding the
24 genetic programmability of lactobacilli for healthcare applications.

25

26 **INTRODUCTION**

27 Lactobacilli are gram-positive rod-shaped lactic acid bacteria (LAB), typically found in
28 humans and animals as commensals. Their stress tolerant phenotypic traits allow them
29 to colonize a wide range of host microenvironments, like the gut, skin, vagina, nasal and
30 oropharyngeal cavity (Ma *et al.*, 2012; Turrone *et al.*, 2014) often providing health
31 benefits in the form of anti-inflammatory, anti-pathogenic and immunomodulatory
32 activities (Darby and Jones, 2017; Bibalan *et al.*, 2017). Due to this, they are one of the
33 largest classes of probiotics and several species are being clinically tested for treating a
34 variety of diseases like ulcerative colitis (Zocco *et al.*, 2006), mastitis (Jiménez *et al.*,
35 2008), atopic dermatitis (Rosenfeldt *et al.*, 2003), bacterial vaginosis (Mastromarino *et*
36 *al.*, 2009) and periodontitis (Teughels *et al.*, 2013). Apart from their health benefits,
37 lactobacilli are also vital for numerous fermentation processes in the food industry, for
38 example in the production of yogurt (Ashraf and Shah, 2011), cheese (Kasimoğlu *et al.*,
39 2004), sourdough bread (Plessas *et al.*, 2008), beer (Chan *et al.*, 2019) and wine (du
40 Toit *et al.*, 2011). Due to this ubiquity in our lives, there is considerable interest to
41 genetically enhance and expand the capabilities of these bacteria for healthcare
42 applications (Pedrolli *et al.*, 2019). For instance, lactobacilli are being engineered as live
43 biotherapeutic products (LBPs) that produce and deliver drugs right at the site of
44 diseases like ulcerative colitis (de Vos, 2011), Human Immunodeficiency Virus (HIV)

45 infection (Watterlot *et al.*, 2010) and respiratory infections (Janahi *et al.*, 2018). They are
46 also prominent candidates for the development of mucosal vaccines in which they are
47 engineered to either display heterologous antigens on their surface or to secrete them
48 (LeCureux and Dean, 2018). These food-grade *Lactobacillus* vaccine vectors would be
49 cheap to produce and can be easily administered orally or intranasally, improving the
50 ability to deploy them both in humans and animals. Examples of infectious diseases
51 against which such vaccines are under development include anthrax, infantile diarrhea,
52 pneumonia and viral infections like, HIV, HPV, influenza and coronavirus (LeCureux
53 and Dean, 2018; Wang *et al.*, 2020). Finally, to track these therapeutic bacteria within
54 the body and study their colonization and clearance profiles, there is considerable
55 interest to make them express reporter proteins that can be imaged *in situ* (Landete *et*
56 *al.*, 2015; Salomé-Desnoullez *et al.*, 2021).

57 Despite such potential, the main limitations for engineering lactobacilli are the
58 scarcity of well-characterized genetic parts and insufficient understanding of
59 biochemical pathways required to build the type of genetic circuits that have been
60 demonstrated in *E. coli* (Elowitz and Leibler, 2000; Wang *et al.*, 2011) and *B. subtilis*
61 (Courbet *et al.*, 2015; Castillo-Hair *et al.*, 2019) . Over two decades of painstaking
62 investigation and screening across phylogenetically close bacteria have generated a
63 handful of reliable parts for use in lactobacilli such as constitutive and inducible
64 promoters, operators, replicons, retention-modules, signal peptides etc. Most of
65 these have been developed in a few species that were found to be amenable to
66 genetic modification, among which *Lactiplantibacillus plantarum* (Zheng *et al.*, 2020)
67 is widely reported (Siezen and van Hylckama Vlieg, 2011). While genomic

68 integration of genes has been demonstrated in these bacteria, the greatest
69 versatility of functions has been achieved using plasmids. Excellent progress has
70 been made in establishing plasmid backbones with low, medium and high copy
71 number replicons (Tauer *et al.*, 2014) , constitutive promoters with a wide range of
72 expression strengths (Rud *et al.*, 2006), a few inducible promoters that can be
73 triggered by peptides (Halbmayr *et al.*, 2008) or sugars (Heiss *et al.*, 2016), signal
74 peptides sequences enabling protein secretion (Mathiesen *et al.*, 2009) or surface
75 display (Mathiesen *et al.*, 2020) and food-grade plasmid retention systems based on
76 resistance to external stressors (e.g. bacteriocins) (Takala and Saris, 2002; Allison
77 and Klaenhammer, 1996) or auxotrophy complementation requiring genomic
78 knockout of a metabolic gene and providing it in the plasmid (Nguyen *et al.*, 2011;
79 Chen *et al.*, 2018). However, the available set of well-characterized genetic parts is
80 still minuscule compared to the toolbox of *E. coli* and needs to be expanded in order
81 to improve the performance and versatility of *Lactobacillus* engineering for
82 healthcare applications.

83 In this work, we introduce 2 new versatile and powerful genetic parts to expand the
84 capabilities of *Lactobacillus* engineering - (i) a novel constitutive promoter from a
85 phylogenetically distant *Salmonella* species that drive protein expression at levels
86 considerably higher than previously reported strong *L. plantarum* promoters and (ii)
87 toxin-antitoxin systems as an alternative strategy for plasmid retention that does not
88 require manipulating the bacterial genome. Unique features of the novel promoter
89 sequence are discussed, which can lead to new design criteria for improving
90 promoter strengths in lactobacilli. The toxin-antitoxin systems introduce a thus-far

91 unexplored modality of plasmid retention in lactobacilli that enables the generation
92 of temporary Genetically Engineered Microorganisms (GEMs), desirable for medical
93 and food-grade applications. These parts and the fundamental insights gained in
94 their characterization will strongly aid in expanding the genetic programmability of
95 lactobacilli.

96

97 **MATERIALS AND METHODS**

98 **Strain, Media and Plasmids**

99 *L. plantarum* WCFS1 was used as the parent strain for promoter strength and
100 plasmid retention characterization. The strain was maintained in the De Man,
101 Rogosa and Sharpe (MRS) media. The culture media, antibiotics and
102 complementary reagents were purchased from Carl Roth GmbH, Germany. Growth
103 media was supplemented with 10 µg/mL of erythromycin to culture engineered *L.*
104 *plantarum* WCFS1 strains. The plasmids pSIP403 and pLp_3050sNuc used in this
105 study were a kind gift from Prof. Lars Axelsson (Addgene plasmid # 122028) (Sørvig
106 *et al.*, 2005a) and Prof. Geir Mathiesen (Addgene plasmid # 122030) (Mathiesen *et*
107 *al.*, 2009) respectively. The plasmid pTlpA39-Wasabi was a kind gift from Prof.
108 Mikhail Shapiro (Addgene plasmid # 86116) (Piraner *et al.*, 2017). The plasmid
109 pUC-GFP-AT was a kind gift from Prof. Chris Barnes (Addgene plasmid # 133306)
110 (Fedorec *et al.*, 2019). The sequence verified genetic constructs created in this
111 study have been maintained in *E. coli* DH5α.

112

113 **Molecular Biology**

114 The genetic constructs developed in this study are based on the pLp3050sNuc/
115 pSIP403 vector backbone. The HiFi Assembly Master Mix, Quick Blunting Kit and
116 the T4 DNA Ligase enzyme were purchased from New England BioLabs (NEB,
117 Germany). PCR was performed using Q5 High Fidelity 2X Master Mix (NEB) with
118 primers purchased from Integrated DNA Technologies (IDT) (Leuven, Belgium).
119 Oligonucleotide gene fragments were purchased as eBlocks from IDT (Coralville,
120 USA). These were codon optimized for maximal expression in the host strain using
121 the IDT Codon Optimization Tool (Coralville, USA). Plasmid extraction and DNA
122 purification were performed using kits purchased from Qiagen GmbH (Hilden,
123 Germany) and Promega GmbH (Walldorf, Germany) respectively. The general
124 schematic of plasmid construction for this study has been shown in Supplementary
125 Figure S1. The promoter sequences used in this study are provided in
126 Supplementary Table S1 and the nucleotide sequences of the toxin-antitoxin
127 modules have been highlighted in Supplementary Table S2.

128 ***L. plantarum* WCFS1 Competent Cell Preparation and DNA Transformation**

129 A single colony of *L. plantarum* WCFS1 was inoculated in 5 mL of MRS media and
130 cultured overnight at 37 °C with shaking (250 rpm). The primary culture was diluted
131 in a 1:50 (v/v) ratio in a 25 mL secondary culture composed of MRS media and 1%
132 (w/v) glycine premixed in a 4:1 ratio. The secondary culture was incubated at 37 °C,
133 250 rpm until OD₆₀₀ reached 0.8, following which the cells were pelleted down by
134 centrifuging at 4000 rpm (3363 × g) for 10 min at 4°C. The pellet was washed twice

135 with 5 mL of ice-cold 10 mM MgCl₂ and then washed twice with 5 mL and 1 mL of
136 ice-cold Sac/Gly solution [10% (v/v) glycerol and 1 M sucrose mixed in a 1:1 (v/v)
137 ratio] respectively. Finally, the residual supernatant was discarded, and the pellet
138 resuspended in 500 µL of Sac/Gly solution. The competent cells were then
139 dispensed in 60 µL aliquots for DNA transformation. For all transformations, 1 µg of
140 dsDNA were added to the competent cells and then transferred to chilled 2 mm gap
141 electroporation cuvettes (Bio-Rad Laboratories GmbH, Germany). Electroporation
142 transformation was done with a single pulse at 1.8 kV, after which 1 mL of lukewarm
143 MRS media was immediately added. The mixture was kept for incubation at 37 °C,
144 250 rpm for a recovery period of 3 h. Following the recovery phase, the cells were
145 centrifuged at 4000 rpm (3363 × g) for 5 min, 800 µL of the supernatant discarded,
146 and 200 µL of the resuspended pellet was plated on MRS Agar supplemented with
147 10 µg/mL of Erythromycin. The plates were incubated at 37 °C for 48 h to allow the
148 growth of distinct single colonies.

149 **Direct cloning in *L. plantarum* WCFS1**

150 To obtain sufficient plasmid quantities (~1 µg) for transformation in *L. plantarum*
151 WCFS1, a modified direct cloning method (Spath *et al.*, 2012) involving PCR-based
152 amplification and circularization of recombinant plasmids was used. Plasmids were
153 constructed and transformed directly in *L. plantarum* WCFS1 strain using a DNA
154 assembly method. Complementary overhangs for HiFi Assembly were either
155 created using PCR primers or synthesized as custom designed eBlocks. Purified
156 overlapping DNA fragments were mixed with the HiFi DNA Assembly Master Mix
157 and assembled as recommended in the standard reaction protocol from the

158 manufacturer. The assembled DNA product was then exponentially amplified by
159 another round of PCR using a pair of primers annealing specifically to the insert
160 segment. 5 µl of the HiFi assembly reaction was used as a template for this PCR
161 amplification of the assembled product (100 µl final volume). The purified PCR
162 product was then subjected to phosphorylation using the Quick Blunting Kit. 2000
163 ng of the purified PCR product was mixed with 2.5 µl of 10X Quick blunting buffer
164 and 1 µl of Enzyme Mix (Milli-Q water was added up to 25 µl). The reaction was
165 incubated first at 25 °C for 30 minutes and then at 70 °C for 10 minutes for enzyme
166 inactivation. Next, phosphorylated products were ligated using the T4 ligase
167 enzyme. 6 µl of the phosphorylated DNA was mixed with 2.5 µl of 10X T4 Ligase
168 Buffer and 1.5 µl of T4 Ligase enzyme (Milli-Q water was added up to 25 µl). Two
169 ligation reactions were performed per cloning (25 µl each). The respective reactions
170 were incubated at 25 °C for 2 hours and then at 70 °C for 30 min for enzyme
171 inactivation. The ligated reactions were mixed together and purified. In order to
172 concentrate the final purified product, three elution rounds were performed instead
173 of one. Each elution was based on 10 µl of Milli-Q water. The concentration of the
174 ligated purified product was measured using the NanoDrop Microvolume UV-Vis
175 Spectrophotometer (ThermoFisher Scientific GmbH, Germany). Finally, 1000 ng of
176 the ligated product were transformed into *L. plantarum* WCFS1 electrocompetent
177 cells, resulting in a transformation efficiency of $2 - 3 \times 10^2$ cfu/µg.

178 Notably, since *L. plantarum* harbors 3 endogenous plasmids (Van Kranenburg *et al.*,
179 2005), sequencing was performed on PCR amplified sections. In detail, colonies of
180 interest were inoculated in MRS supplemented with 10 µg/mL of Erythromycin and

181 grown overnight at 37 °C. The following day, 1 mL of the culture was pelleted down,
182 and the supernatant was discarded. Next, a tip was used to collect a tiny part of the
183 pellet, which was used as a template for PCR (100 µL final volume). Finally, PCR
184 products were purified and sent for Sanger sequencing to Eurofins Genomics
185 GmbH (Ebersberg, Germany) by opting for the additional DNA purification step.

186 **Microplate reader Setup for Thermal Gradient Analysis**

187 Bacterial cultures were cultivated in 5 mL of MRS media (supplemented with 10
188 µg/mL erythromycin) at 30°C with continuous shaking (250 rpm). The following day,
189 cultures were diluted to 0.1 OD₆₀₀ in 3 mL of antibiotic supplemented fresh MRS
190 media and propagated at 30°C, 250 rpm. At OD₆₀₀ = 0.3, the cultures were
191 dispensed into Fisherbrand™ 0.2mL PCR Tube Strips with Flat Caps (Thermo
192 Electron LED GmbH, Germany) and placed in the Biometra Thermocycler (Analytik
193 Jena. GmbH, Germany). For the P_{spp}-mCherry construct, 25 ng/mL of the 19 amino
194 acid Sakacin P inducer peptide (Spplp) with the sequence NH₂-
195 MAGNSSNFIHKIKQIFTHR-COOH (GeneCust, France) was added to the culture
196 and thoroughly vortexed before preparing the aliquots. The thermal assay was set
197 at a temperature gradient from 31°C to 41°C with regular increment of 2°C. The lid
198 temperature was set at 50°C to prevent the evaporation of the liquid and maintain a
199 homogeneous temperature in the spatially allocated PCR tubes. After a time interval
200 of 18 h, the PCR strips were centrifuged in a tabletop minicentrifuge (Biozym
201 GmbH, Germany) to pellet down the cells and discard the supernatant. The cells
202 were then resuspended in 200 µL of 1X PBS and added to the clear bottom 96-well
203 microtiter plate (Corning® 96 well clear bottom black plate, USA). The samples

204 were then analyzed in the Microplate Reader Infinite 200 Pro (Tecan Deutschland
205 GmbH, Germany) and both the absorbance (600 nm wavelength) and mCherry
206 fluorescence intensity ($Ex_{\lambda} / Em_{\lambda} = 587 \text{ nm}/625 \text{ nm}$) were measured. The z-position
207 and gain settings for recording the mCherry fluorescent intensity were set to 19442
208 μm and 136 respectively. Fluorescence values were normalized with the optical
209 density of the bacterial cells to calculate the Relative Fluorescence Units (RFU)
210 using the formula $RFU = \text{Fluorescence}/OD_{600}$.

211 **Fluorescence Microscopy Analysis**

212 Bacterial cultures were grown overnight in 5 mL of MRS media (supplemented with
213 10 $\mu\text{g}/\text{mL}$ erythromycin) at 37°C with continuous shaking (250 rpm). The following
214 day, the OD_{600} of the P_{spp} -mCherry construct was measured and subcultured at
215 $OD_{600} = 0.01$. When the P_{spp} -mCherry bacterial culture reached $OD_{600} = 0.3$, it was
216 induced with 25 ng/mL of Spplp and the remaining constructs were subcultured in
217 fresh media at 0.01 OD_{600} . All the cultures were then allowed to grow for 18 h under
218 the same growth conditions (37°C, 250 rpm) to prevent any heterogeneity in
219 promoter strength expression due to differential growth parameters. Later, 1 mL of
220 the cultures were harvested by centrifugation (15700 $\times g$, 5 min, 4 °C), washed
221 twice with Dulbecco's 1X PBS (Phosphate Buffer Saline) and finally resuspended in
222 1 mL of 1X PBS. 10 μL of the suspensions were placed on glass slides of 1.5 mm
223 thickness (Paul Marienfeld GmbH, Germany) and 1.5H glass coverslips (Carl Roth
224 GmbH, Germany) were placed on top of it. The samples were then observed under
225 the Plan Apochromat 100X oil immersion lens (BZ-PA100, NA 1.45, WD 0.13 mm)
226 of the Fluorescence Microscope BZ-X800 (Keyence Corporation, Illinois, USA). The

227 mCherry signal were captured in the BZ-X TRITC filter (model OP-87764) at
228 excitation wavelength of 545/25 nm and emission wavelength of 605/70 nm with a
229 dichroic mirror wavelength of 565 nm. The images were adjusted for identical
230 brightness and contrast settings and were processed with the Fiji ImageJ2
231 software.

232 **Flow Cytometry Analysis**

233 Quantification of fluorescent protein expression levels of the strains were performed
234 using Guava easyCyte BG flow-cytometer (Luminex, USA). Bacterial cultures
235 subjected to the same treatment conditions mentioned above were used for Flow
236 Cytometry analysis. 1 mL of the bacterial suspensions were harvested by
237 centrifugation at 13000 rpm (15700 × g). The supernatant was discarded and the
238 pellet was resuspended in 1 mL of sterile Dulbecco's 1X PBS. The samples were
239 then serially diluted by a 10⁴ Dilution Factor (DF) and 5,000 bacteria events were
240 recorded for analysis. Experiments were performed in triplicates on three different
241 days. During each analysis, the non-fluorescent strain carrying the empty vector
242 was kept as the negative control. A predesigned gate based on forward side scatter
243 (FSC) and side scatter (SSC) thresholding was used to remove debris and doublets
244 during event collection and analysis. mCherry fluorescence intensity was measured
245 using excitation by a green laser at 532 nm (100 mW) and the Orange-G detection
246 channel 620/52 nm filter was used for signal analysis. The gain settings used for the
247 data recording were, Forward Scatter (FSC) – 11.8; Side Scatter (SSC) - 4, and
248 Orange-G Fluorescence – 1.68. The compensation control for fluorescence

249 recording was set at 0.01 with an acquisition rate of 5 decades. Data analysis and
250 representation were done using the Luminex GuavaSoft 4.0 software for EasyCyte.

251 **Toxin/Antitoxin Module based Plasmid Construction**

252 Similar to previous reports in *E. coli* (Fedorec *et al.*, 2019), the effect of Txe/Axe
253 (toxin/antitoxin) module from *E. faecium* (Grady and Hayes, 2003) was tested in *L.*
254 *plantarum* WCFS1 to test its capability for antibiotic-free plasmid retention. TA
255 Finder version 2.0 tool (Xie *et al.*, 2018) was used to select further type-II TA
256 (Toxin/Antitoxin) systems present in *Lactobacillus* genomes. *L. acidophilus*, *L.*
257 *crispatus*, *L. casei*, *L. reuteri*, and *L. plantarum* WCFS1 genomes were retrieved
258 from NCBI Genome. TA systems harbored within these genomes were mined using
259 the default parameters of TA Finder. Only TA systems annotated by NCBI BlastP
260 were selected as test candidates. The TA systems YafQ/DinJ, HicA/HicB,
261 HigB/HigA, MazF/MazE from *L. casei*, *L. acidophilus* and *L. plantarum* WCFS1 were
262 selected for further testing and analysis.

263 Txe/Axe system was amplified by PCR from the plasmid pUC-GFP-AT (Fedorec *et*
264 *al.*, 2019). DinJ/YafQ and HicA/HicB systems were synthesized as custom-designed
265 eBlocks. HigA/HigB and MazE/MazF were amplified from the genome of *L.*
266 *plantarum* WCFS1. TA systems were inserted into the P_{tlpA} -mCherry plasmid,
267 generating the plasmids P_{tlpA} -mCherry-Txe/Axe, P_{tlpA} -mCherry-YafQ/DinJ, P_{tlpA} -
268 mCherry-HicA/HicB, P_{tlpA} -mCherry-HigB/HigA, P_{tlpA} -mCherry-MazF/MazE For
269 constructing the combinatorial TA module (P_{tlpA} -mCherry Combo), the best
270 performing endogenous and non-endogenous TA systems recorded after 100

271 generations (MazF/MazE and YafQ/DinJ) were subcloned and integrated into the
272 same plasmid in reverse orientations.

273 **TA Mediated Plasmid Retention Analysis**

274 The TA module containing constructs were inoculated in 5 mL cultures of 10 µg/mL
275 erythromycin supplemented MRS media and incubated overnight at 37°C with
276 continuous shaking (250 rpm). The following day, the constructs were subcultured
277 at an initial OD₆₀₀ = 0.01 in fresh MRS media (both with and without antibiotic
278 supplementation). The bacterial cultures were incubated for 12 consecutive days
279 with a daily growth period of 24 h ensuring an average of ~8 generations per day,
280 until crossing the final threshold of 100 generations. Sample preparation for flow
281 cytometry analysis was conducted according to the protocol mentioned before. The
282 mCherry positive cell population directly correlated to the bacterial population
283 retaining the engineered plasmid. The entire experiment was repeated in biological
284 triplicates.

285 To cross-check the flow cytometry analysis, the bacterial cultures grown for 100
286 generations without antibiotic supplementation were centrifuged and resuspended in
287 1 mL of sterile Dulbecco's 1X PBS. The resuspended bacterial solutions were
288 diluted (DF=10⁶) and plated on MRS Agar plates supplemented without antibiotic
289 and incubated in a static incubator for 48 h. The plates were then imaged using the
290 GelDocumentation System Fluorchem Q (Alpha Innotech Biozym GmbH, Germany)
291 both in the Ethidium Bromide channel (Ex_λ/Em_λ = 300 nm/600 nm) and Cy3
292 channel (Ex_λ/Em_λ = 554 nm/568 nm) to visualize the cell population producing

293 mCherry fluorescence. The fluorescent bacterial subpopulation on the non-selective
294 MRS agar medium correlated to the plasmid retention frequency of the respective
295 TA systems in the absence of selection pressure.

296 **Growth Rate Measurements**

297 For studying the influence of the heterologous protein production and toxin-antitoxin
298 modules on the bacterial growth rate, bacterial cultures were cultivated overnight in
299 antibiotic supplemented MRS media at 37°C with continuous shaking (250 rpm).
300 Following day, the bacterial cultures were subcultured in secondary cultures at an
301 initial $OD_{600} = 0.01$. After 4 h incubation at 37°C, the OD_{600} of the cultures reached
302 0.1 and 200 μ L of the cultures were distributed in UV STAR Flat Bottom 96 well
303 microtiter plates (Greiner BioOne GmbH, Germany). The 96 well assay plate was
304 placed in the Microplate Reader with constant shaking conditions at an incubation
305 temperature of 37°C. The kinetic assay was set to record the absorbance of the
306 bacterial cultures at 600 nm wavelength with an interval of 10 min for an 18 h time
307 duration. The experiment was conducted in triplicates on three independent days.

308

309 **Bioinformatic analysis**

310 All genome sequence included in the phylogenetic analysis were retrieved from
311 NCBI Genome. The phylogenetic tree was built using the web server for genome-
312 based prokaryote taxonomy “Type (Strain) Genome Server” (TYGS), restricting the
313 analysis only to the sequences provided (Meier-Kolthoff and Göker, 2019). The
314 Genome BLAST Distance Phylogeny (GBDP) tree, based on 16S rDNA gene

315 sequences, was obtained. The Interactive Tree of Life (iTOL) tool was used for the
316 display, annotation, and management of the phylogenetic tree (Letunic and Bork,
317 2007).

318 For the multiple sequence alignment, protein sequences of the $\sigma 70$ subunits from *L.*
319 *plantarum*, *E. coli* and *S. typhimurium* RNA polymerases were first retrieved from
320 Uniprot . Sequences were aligned using the tool MUSCLE (Edgar, 2004). Jalview
321 was used to visualize and edit the multiple sequence alignment (Waterhouse *et al.*,
322 2009).

323 SnapGene was used to identify DNA sequences similar to P_{tpA} within the genome of
324 *L. plantarum* WCFS1 using the feature “Find Similar DNA Sequences”. The search
325 allowed a mismatch or gap/insertion every 4 bases. BPPROM, an online tool for
326 predicting bacterial promoters, was used to identify the -35 and -10 boxes within this
327 promoter (Madeira *et al.*, 2022). BlastP was used to identify the protein encoded by
328 the gene driven by this promoter. Promoter alignment was performed using
329 MUSCLE (Edgar, 2004).

330

331 RESULTS AND DISCUSSIONS

332 ***P*_{tpA} Promoter from Salmonella drives high-level constitutive expression**

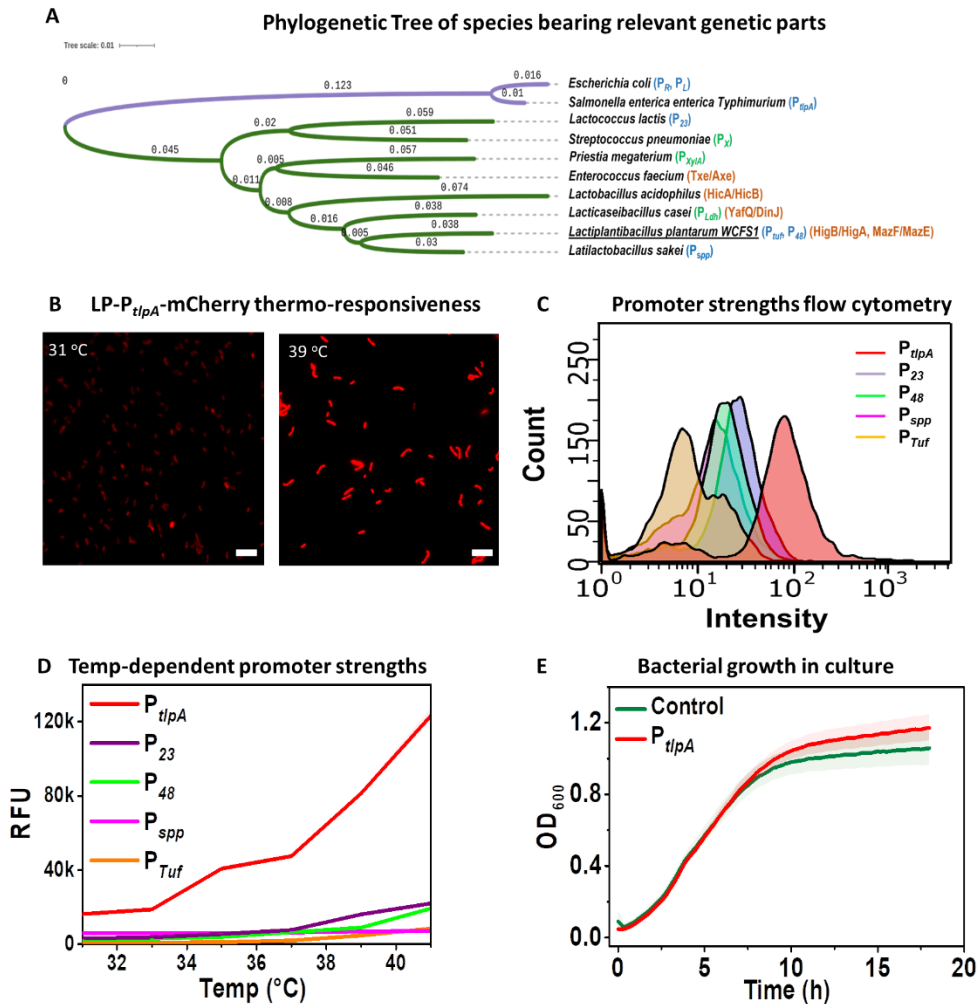
333 The strongest promoters in lactobacilli have been found by either screening the
334 genome of the host strain (Rud *et al.*, 2006; Bron *et al.*, 2004) or adapting those
335 driving high-level protein expression in phylogenetically close lactic acid bacteria

336 (Russo *et al.*, 2015) (Figure 1A). In the few reports where promoters from
337 phylogenetically distant species like *P. megaterium* (P_{xyIA}) or *E. coli* (P_{T7} from
338 lambda phage) (Heiss *et al.*, 2016) have been tested, expression levels were found
339 to be comparatively low. Contrary to this trend, we serendipitously stumbled upon a
340 promoter (P_{tIpA}) from the phylogenetically distant gram-negative *Salmonella*
341 *typhimurium* (Figure 1A) capable of driving protein expression at levels higher than
342 previously reported strong promoters in *L. plantarum* WCFS1. In *Salmonella*, P_{tIpA}
343 along with its repressor is capable of thermo-responsively regulating gene
344 expression and this functionality had been previously transferred to *E. coli* for
345 therapeutic purposes (Piraner *et al.*, 2017; Hurme *et al.*, 1997). To test whether the
346 P_{tIpA} promoter would be a suitable candidate for driving transcription in *L. plantarum*,
347 a fluorescent reporter protein (mCherry) was cloned downstream of this promoter.
348 The promoter surprisingly seemed to constitutively drive a high-level of protein
349 expression with a mild degree of thermal regulation (<5-fold increase from 31 °C to
350 39 °C) (Figure 1B). Next the repressor based thermo-responsive functionality was
351 tested in *L. plantarum*, by creating the pTIpA39 plasmid, with the P_{tIpA} promoter
352 driving expression of mCherry and the codon optimized TIpA repressor being
353 expressed constitutively by the P_{48} promoter (Rud *et al.*, 2006). However, the
354 pTIpA39 plasmid showed no significant repression of mCherry at lower temperature
355 gradients in comparison to its repressor-free counterpart (Supplementary Figure
356 S2D). Most remarkably, flow cytometry and fluorescence spectroscopy analysis
357 revealed that mCherry expression levels driven by the P_{tIpA} promoter significantly
358 exceeded the levels driven by some of the strongest promoters previously reported

359 in *L. plantarum* - P_{23} (Meng *et al.*, 2021), P_{48} (Rud *et al.*, 2006), P_{spp} (Sørvig *et al.*,
360 2003) and P_{Tuf} (Spangler *et al.*, 2019) (Figure 1C, Supplementary S3A). At 31 °C,
361 mCherry expression levels were at least 2-fold higher than these other promoters,
362 while this increased to 5-fold at 39 °C (Figure 1D, Supplementary Figure S3B). All
363 constitutive promoters (P_{23} , P_{48} , P_{Tuf}) were mildly thermo-responsive, while the
364 inducible promoter (P_{spp}) was not (Supplementary Figure S4A). To check whether
365 such high gene expression can be driven by other phylogenetically distant thermo-
366 responsive promoters, we tested the well-known heat inducible pR and pL
367 promoters from *E. coli* lambda phage. However, only low levels of mCherry
368 expression were observed with these promoters (Supplementary Figure S2A,
369 Supplementary S2B). Fluorescence spectroscopy revealed that the strength of the
370 P_{tipA} promoter at 37 °C was 26- and 39-fold higher than the pR and pL promoter,
371 respectively (Supplementary Figure S2C).

372 Another important factor for high-level gene expression driven by P_{tipA} is that the
373 spacer length between the ribosome binding site (RBS, 5'-AGGAGA-3') and the
374 start codon needs to be different in *L. plantarum* compared to *E. coli*. In *E. coli* this
375 spacer length of 6 bp has been previously reported (Piraner *et al.*, 2017; Kan *et al.*,
376 2020; Chee *et al.*, 2022; Rottinghaus *et al.*, 2022), whereas in *L. plantarum* a 9 bp
377 spacer improves expression levels by 25-fold compared to a 6 bp spacer
378 (Supplementary Figure S4B), in accordance with previous reports (Tauer *et al.*,
379 2014). Despite the high level of protein expression driven by P_{tipA} with a 9 bp
380 spacer, the growth rate of this strain at 37 °C was similar to that of the empty vector

381 control strain, suggesting that this protein overexpression did not metabolically
 382 overburden the cell (Figure 1E).



383

384 **Figure 1.** (A) Phylogenetic tree highlighting the distances between species from
 385 which various genetic parts have been tested in *L. plantarum*. Purple clade
 386 corresponds to Gram-negative bacteria. Green clade corresponds to Gram-positive
 387 bacteria. Promoters tested in this study are labelled in blue. Promoters tested by
 388 others in *L. plantarum* are labelled in green. Orange labels correspond to the TA
 389 systems tested in this study. (B) Fluorescence microscopy of P_{tlpA} driven mCherry
 390 expression in *L. plantarum* WCFS1 cultivated at 31°C and 39°C for 18 h. Scale bar
 391 = 10 μm (C) Flow Cytometry analysis of P_{tlpA}, P₂₃, P₄₈, P_{spp} and P_{Tuf} driven mCherry
 392 expression in *L. plantarum* WCFS1 after 18 h incubation at 37°C. (D) Fluorescence
 393 spectroscopy analysis of the P_{tlpA}, P₂₃, P₄₈, P_{spp} and P_{Tuf} driven mCherry expression
 394 after 18 h incubation at temperatures ranging from 31°C to 41°C. (E) Growth rate

395 (OD₆₀₀) measurement of *L. plantarum* WCFS1 strains containing a control plasmid
396 and P_{tlpA}-mCherry for 18 h at 37°C. In (C) and (D), the solid lines represent mean
397 values, and the lighter bands represents standard deviations calculated from three
398 independent biological replicates.

399

400 To understand why P_{tlpA} drives gene expression in *L. plantarum*, we looked into its
401 function in Salmonella, where it is a promoter of the σ 70 sigma factors. (Dawoud et
402 al., 2017). This family of sigma factors is involved in regulating the expression of
403 housekeeping genes in most prokaryotes, including lactobacilli (Todt *et al.*, 2012).
404 Multiple Sequence Alignment (MSA) among the major RNA polymerase σ 70
405 proteins (RpoD) of *E. coli*, *S. typhimurium*, and *L. plantarum* strains (Figure 2A)
406 revealed significant similarity between the domain-2 and domain-4 regions,
407 responsible for binding to the -10 and -35 regions of the promoter during
408 transcription initiation. Interestingly, Gaida *et al.*, (2015) showed that, when
409 expressed in *E. coli*, the *L. plantarum* RpoD can recruit *E. coli*'s RNA polymerase to
410 initiate transcription from a wide variety of heterologous promoters. Compared to
411 sigma factors from six other bacteria, they found that the *L. plantarum* RpoD was
412 the most promiscuous and helped to enlarge the genomic space that can be
413 sampled in *E. coli*. These analyses explain why the P_{tlpA} promoter from a
414 phylogenetically distant species functions in *L. plantarum* but does not necessarily
415 reveal how it drives such high expression levels compared to previously reported
416 promoters.

417 To understand this, we investigated aspects of P_{tlpA}'s sequence (Figure 2B). One
418 unique characteristic is that it harbors the sigma70 consensus sequence at the -10

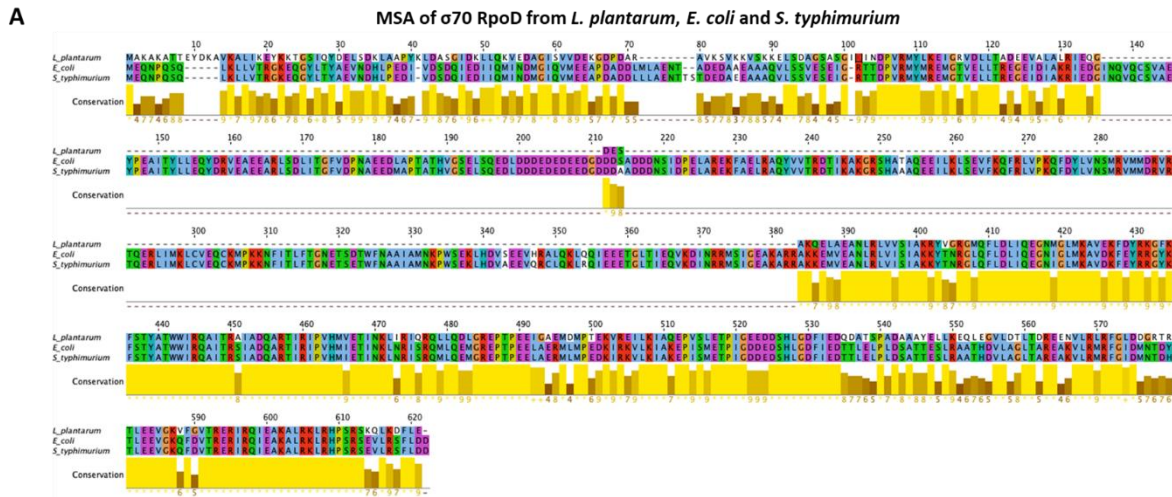
419 region (5'-TATAAT-3') but not at the -35 region (5'-TTGACA-3') (Todt et al., 2012).
420 Based on previous reports in gram positive bacteria like *B. subtilis* (Helmann et al.,
421 1995), it is possible that the deviation from the consensus -35 sequence can be
422 compensated for the presence of the conserved dinucleotide "TG" sequence at the -
423 14 and -15 position of the P_{tlpA} promoter. It has been shown that the presence of
424 this sequence upstream of the -10 region in the promoter can mediate rapid
425 promoter melting during transcription initiation and upregulate the transcription rate
426 of corresponding genes. However, most of the promoters reported by Rud et al.
427 (Rud et al., 2006) for *L. plantarum*, also have the conserved "TG" dinucleotide at the
428 -15 position of the promoter. When the strength of the strongest promoter in that
429 library (P_{48}) was compared to the P_{tlpA} promoter, the mCherry production rate by the
430 P_{tlpA} promoter was significantly higher. This suggests that the P_{tlpA} promoter must
431 have additional reasons that contribute to its exceptional performance in *L.*
432 *plantarum* WCFS1.

433

434 More interestingly, the whole promoter sequence contains no cytosine (C) bases, in
435 contrast to previously reported in *L. plantarum* promoters, most of which contain 2 to
436 4 cytosine bases in the -35 to -10 region (Rud et al., 2006; Meng et al., 2021; Sørvig
437 et al., 2003; Spangler et al., 2019). Additionally, the spacer between the -35 and -10
438 regions of the P_{tlpA} promoter contains no adenine (A) bases. Notably, A and C bases
439 are susceptible to methylation in bacteria, which has been associated with
440 epigenetic gene regulation (Beaulaurier et al., 2019; Casadesús et al., 2006).
441 However, on analysis of 34 constitutive promoter sequences from the synthetic

442 promoter library reported by Rud *et al.*, (2006) and those tested in this study
443 (Supplementary Table S3), no correlation could be derived between promoter
444 strengths and number of C bases within the -35 to -10 region (Supplementary
445 Figure S6A) or the A bases in the spacer (Supplementary Figure S6B). If
446 methylation could be influencing promoter strengths, it would be necessary to
447 identify the methyltransferase recognition sequences in *L. plantarum* to derive
448 meaningful correlations. We then searched for DNA sequences similar to P_{tlpA} within
449 the genome of *L. plantarum* WCFS1. Out of 6 hits (Supplementary Figure S7A),
450 only one of them was located upstream of a gene that encodes for a known protein
451 (HAMP domain-containing histidine kinase - locus: lp_0282, complement:
452 255805..257181), with a percent identity score of 82.76 compared to P_{tlpA} . This
453 sequence (**GTTTATGTTGGTTATTTACGTAATAAAAT**) was identified as a
454 promoter (referred to as P_{HAMP}) using BPROM, with -35 and -10 regions (in bold)
455 diverging from P_{tlpA} by single bases each (Supplementary Figure S7B). Notably,
456 P_{HAMP} also contains four A bases and one C base in the spacer. When the full
457 promoter sequence (Supplementary Table S1) was cloned upstream of mCherry,
458 only weak expression was observed (Supplementary Figure S7C), suggesting that
459 one or more of these mismatches compared to P_{tlpA} are essential for driving high-
460 level gene expression. These unique features of the P_{tlpA} promoter sequence
461 provide interesting clues for understanding factors affecting promoter strengths in *L.*
462 *plantarum*. To gain deeper insights into P_{tlpA} 's unprecedented strength, further
463 studies analyzing mutant libraries of the promoter and/or measuring DNA
464 methylation patterns are required.

465



466

B P_{tlpA} : 5' TTAATTTGTTTGTAGTTAGTTTATTTGTTGGTTTGTGGTTATAATAT 3'

-35 Spacer -10

467 **Figure 2.** (A) Homology analysis of $\sigma 70$ RpoD genes from *L. plantarum*, *E. coli*, and
 468 *S. typhimurium*. Height and brightness of the yellow bars indicate the extent to
 469 which individual residues are conserved across all 3 bacteria. (B) P_{tlpA} promoter
 470 sequence with -35, spacer and -10 regions labelled

471

472 Toxin/Antitoxin based plasmid retention and transient GEMs

473 Apart from high expression levels, use of lactobacilli for healthcare applications
 474 requires strategies to retain heterologous genes in the engineered bacteria in a
 475 cheap and compatible manner. TA systems ensure plasmid retention in a bacterial
 476 population through a post-segregation killing mechanism. They constitutively
 477 express long-lasting toxins and short-lived antitoxins. As long as the plasmid is
 478 present, sufficient antitoxin is produced to neutralize the corresponding toxin. On
 479 bacterial division, if a daughter cell does not receive any plasmid copies, the
 480 antitoxin rapidly degrades, and the active toxin kills the cell. While TA systems have

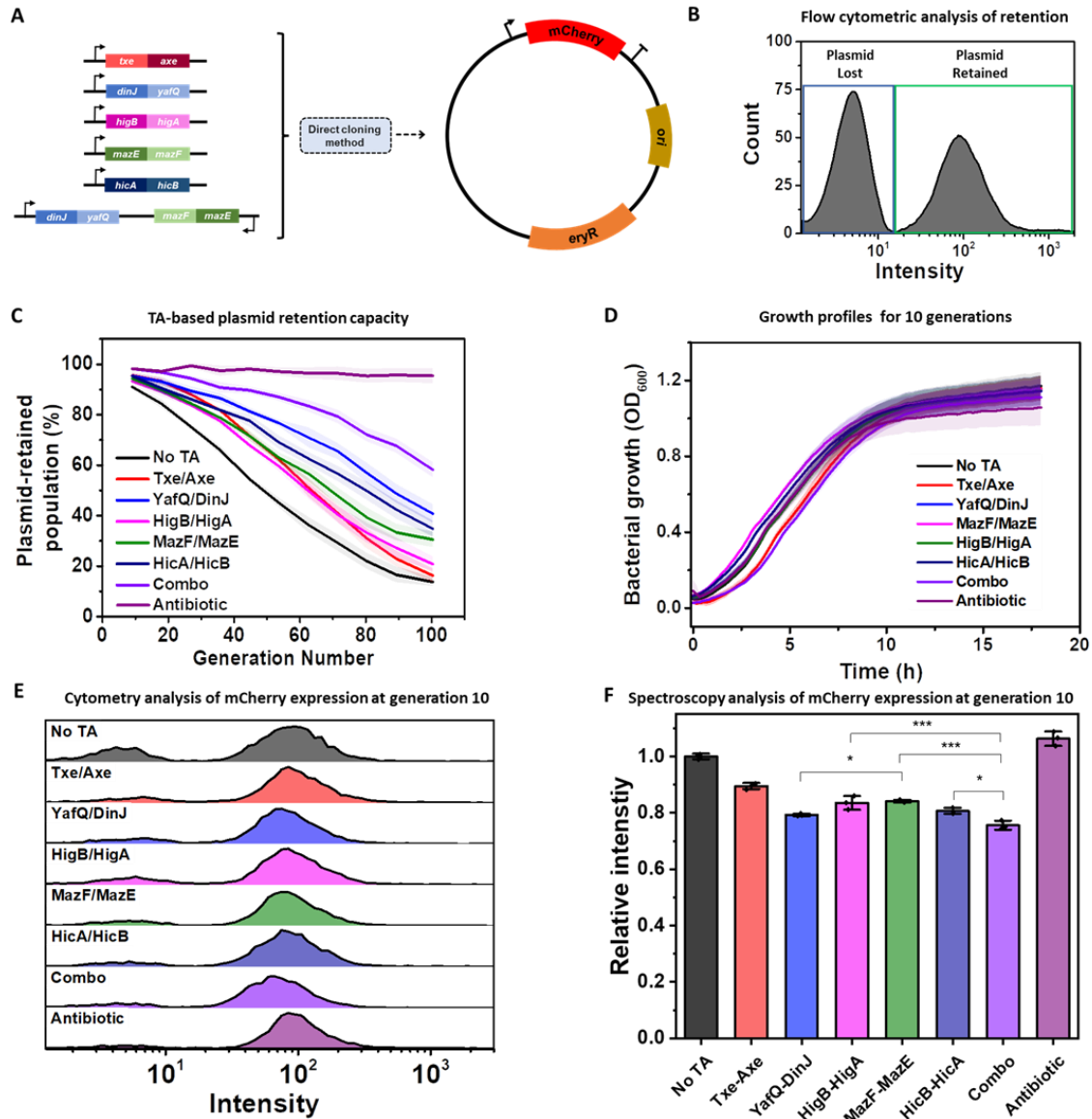
481 been investigated in the past for bioremediation and biotechnology purposes, their
482 applicability was limited by the fact that their plasmid retention efficiency did not
483 match that of antibiotic or auxotrophy based retention systems (Stirling et al., 2020).
484 However, interest in TA systems has reemerged for living therapeutic applications
485 because of 2 reasons – (i) better understanding of TA systems leading to improved
486 efficiencies (Fedorec *et al.*, 2019) and (ii) biosafety features they offer in reducing
487 horizontal gene transfer (Wright *et al.*, 2013). Accordingly, reports have recently
488 emerged where TA systems are showing greater promise for bacteria engineered
489 as live vaccines or drug delivery vehicles (Kan et al., 2020; Abedi *et al.*, 2022).
490 While these demonstrations have been done in *E. coli*, the use of TA system in
491 lactobacilli for plasmid retention has not yet been systematically investigated. From
492 literature reports and using the TA finder bioinformatics tool, we identified and
493 selected 5 different type II TA system (all named as toxin/antitoxin) – (i) Txe/Axe,
494 from *Enterococcus faecium* that was shown to ensure long-term plasmid retention in
495 *E. coli* (Fedorec *et al.*, 2019), (ii) YafQ/DinJ from *L. casei* (Levante *et al.*, 2019), (iii)
496 HigB/HigA and (iv) MazF/MazE from *L. plantarum* WCFS1, and (v) HicA/HicB from
497 *L. acidophilus* (Phylogeny in Figure 1A). In all these systems, the toxin is an
498 endoribonuclease and the antitoxin is its corresponding inhibitory protein. These
499 modules were added to the plasmid encoding P_{tipA} -driven mCherry expression
500 (Figure 3A) and the resultant strain was repeatedly sub-cultured for up to 100
501 generations. Plasmid retention was quantified by determining the proportion of the
502 bacterial population expressing mCherry using flow cytometry and agar plate colony
503 imaging analysis (Supplementary Figure S5B). Notably, the sensitivity of this

504 analysis was greatly improved by the high-level of expression driven by the P_{tlpA}
505 promoter, which enabled clear demarcation of plasmid-retained and plasmid-lost
506 cells (Figure 3B). Such a clear demarcation was not possible with the other
507 promoters, like P_{23} since the fluorescent signal seemed to partially overlap with
508 background signal from non-fluorescent cells (Supplementary Figure S5A). In the
509 absence of a TA system (P_{tlpA} mCherry plasmid), the proportion of plasmid-bearing
510 bacteria steadily declined by about 1%/ generation, ending with ~15% of the
511 population retaining the plasmid after 100 generations (Figure 3C). Compared to
512 this, the Txe/Axe system initially supported better retention with a plasmid loss of
513 about 0.5%/generation for 40 generations, after which this loss accelerated to
514 ~1.2%/generation, ending in ~18% of the population retaining the plasmid after 100
515 generations. HigB/HigA and MazF/MazE systems performed similarly for the most
516 part but provided slightly better retention after 100 generations (20% and 30%
517 respectively). HicA/HicB slowed plasmid loss to 0.5%/generation for 50 generations
518 and 0.8%/ generation, thereafter, resulting in retention level of ~35% after 100
519 generations. Finally, YafQ/DinJ was found to provide the best retention capabilities
520 with plasmid loss of 0.5%/generation for 70 generations and 1%/ generation
521 thereafter, resulting in a retention level of ~40% after 100 generations (Figure 3C).

522 Previous studies have shown that combining different TA systems can cumulatively
523 offer better plasmid retention capabilities (Torres et al., 2003; Bardaji *et al.*, 2019),
524 although this has not been tested in lactobacilli. So, we combined the best-
525 performing TA system endogenous to *L. plantarum* WCFS1 (MazF/MazE) with the
526 best-performing non-endogenous system (YafQ/DinJ) and observed better plasmid

527 retention capabilities with this combination, yielding a slow plasmid loss of
528 0.2%/generation for 50 generations and a gradual increase to 0.8%/generation
529 thereafter, resulting in a considerably higher retention of 60% over 100 generations.
530 Comparatively, plasmids maintained under antibiotic selection pressure were
531 steadily retained at >90% through 100 generations, as expected. In all strains
532 harboring TA modules, bacterial growth rates (Figure 3D) and mCherry expression
533 levels (Figure 3E) were found to be minimally impacted compared to “No TA” or
534 antibiotic-retention conditions over the first 10 generations. These results suggest
535 that the toxins did not drastically impede the regular functioning of the cells.
536 Fluorescence spectroscopy analysis of the liquid cultures after 10 generations
537 (Figure 3F) reveals that the TA modules showing higher efficiency in retaining
538 plasmids in the absence of selection pressure (YafQ/DinJ and combo), have
539 significantly lower intensities of mCherry production in comparison to the other TA
540 candidates. The greatest drop in protein expression (~23%) was observed in the
541 strain harboring the TA combo and could be due to an increase in the plasmid size
542 possibly burdening the cells and maybe even resulting in a minor drop in copy
543 number. However, since The YafQ/DinJ construct also causes a drop of comparable
544 magnitude (~20%), it is possible that the toxin in this system mildly interferes with
545 protein expression, which becomes detectable with the overexpression of mCherry
546 by P_{tIpA} but does not drastically affect growth. Further in depth investigation would
547 be required to identify the specific cause of this effect. However, it must be noted
548 that even with the drop in expression level caused by the combo TA system, P_{tIpA}

549 driven mCherry expression was at least 4-fold higher than that of the next strongest
550 promoter, P₂₃.



551
552

553

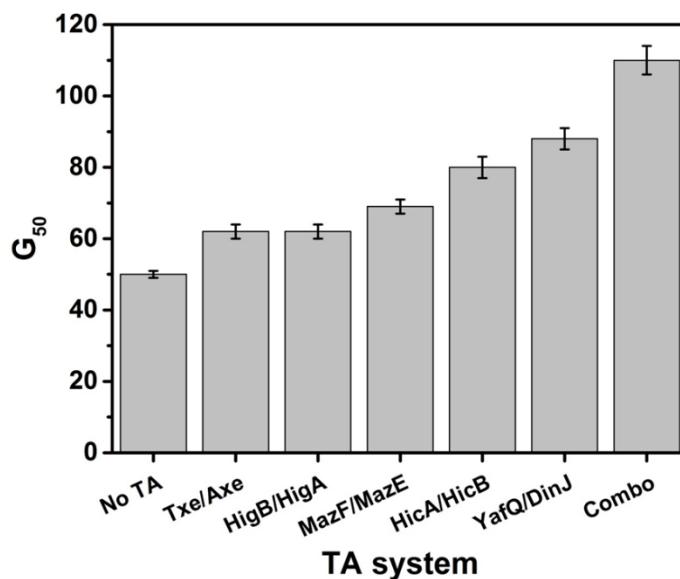
554 **Figure 3.** (A) Schematic Representation of cloning the different TA genetic modules into
555 the P_{tlpA}-mCherry plasmid. (B) Sample flow Cytometry histogram plot of the P_{tlpA}-
556 mCherry plasmid containing strain without any TA module or selection pressure after 50
557 generations of serial passaging in the absence of antibiotic. The green box corresponds

558 to the bacterial population retaining the plasmid and the blue box represents the
559 population devoid of the plasmid. (C) Plasmid retention analysis of the TA module
560 containing strains for 100 generations without antibiotics along with no TA and antibiotic
561 selection pressure conditions for comparison. (D) Growth rate (OD_{600}) of strains with the
562 TA modules, no TA and antibiotic retention over 10 generations at 37°C. In (C) and (D),
563 the solid lines represent mean values and the lighter bands represents SD calculated
564 from three independent biological replicates. Combo = MazF/MazE + YafQ/DinJ . (E)
565 Flow cytometry plots of strains containing TA modules, no TA and antibiotic retention
566 after 10 generations. The Y-axis for each plot represents counts with plot heights in the
567 range of 450 – 500 (F) Fluorescence Spectroscopy analysis of strains containing TA
568 modules, no TA and antibiotic retention after 10 generations. The relative intensity has
569 been plotted for all the TA strains by normalizing their respective fluorescence values
570 against the “No TA” strain. The data represents three independent biological replicates.
571 p-values are calculated using one-way ANOVA with Tukey test on respective means (*
572 $p < 0.05$, *** $p < 0.001$). The “No TA”, “Txe-Axe” and “Antibiotic” conditions are significantly
573 different from other candidates, so their p - values have not been explicitly highlighted.

574

575 It is important to note that a single generation corresponds to a bacterial duplication,
576 so 10 generations = 2^{10} or $\sim 10^3$ bacteria and 100 generations = 2^{100} or $\sim 10^{30}$
577 bacteria from a single cell. Potential applications of lactobacilli for living therapeutics
578 or engineered living materials are not expected to reach such high generation
579 numbers either due to short application time periods (Janahi *et al.*, 2018; LeCureux
580 and Dean, 2018; Wang *et al.*, 2020) or external growth restrictions (Bhusari *et al.*,
581 2022). Thus, the >90% retention levels provided by the combo TA system for up to
582 40 generations should be more than sufficient for these applications. Furthermore,
583 loss of the plasmid only reverts the bacteria to their non-GEM probiotic status, thus
584 enabling the generation of transient GEMs that would be desirable for such
585 applications. Accordingly, by varying the TA system used, the GEM lifetime of these
586 organisms could be tuned. Based on this concept, we introduce a new metric, G_{50} ,
587 for characterizing such transient GEMs. The G_{50} value corresponds to the

588 generation at which half the population of a strain has lost its plasmid. As shown in
589 Figure 4, G_{50} can be tuned from 50 generations for the No TA condition up to 110
590 generations (extrapolated) for the combo system. Further exploration of additional
591 TA systems in future studies will contribute to more fine tuning of retention lifetimes
592 and possibly even lead to near-perfect retention as has been achieved in *E. coli* by
593 the Txe/Axe system (Fedorec *et al.*, 2019). These G_{50} values are expected to
594 depend on culture parameters and environmental factors, due to which it could also
595 become a useful metric for assessing natural and industrial conditions in which
596 lactobacilli grow and function.



597

598 **Figure 4.** G_{50} values of the different TA systems tested in *L. plantarum*. Combo =
599 MazF/MazE + YafQ/DinJ

600

601 **CONCLUSIONS**

602 Lactobacilli as probiotics and commensals in humans and animals have immense
603 potential to be developed for healthcare applications but as non-model organisms,
604 have very poorly equipped genetic toolboxes. Addressing this limitation, this study
605 describes two new genetic modules, characterized in probiotic *L. plantarum* – an
606 ultra-strong constitutive promoter (P_{tIpA}) and TA plasmid retention systems. Our
607 results demonstrate that the promoter drives gene expression at levels over 5-fold
608 higher than the strongest promoters previously reported in *L. plantarum* and the TA
609 systems decelerate plasmid loss in a tunable manner without the need for external
610 selection pressures or genomic manipulations.

611 Apart from the impact, these modules will have in expanding the programmability of
612 lactobacilli, the unique conceptual insights gained from this work will aid in the
613 further development of genetic parts. For one, the unique features of the P_{tIpA}
614 promoter sequence that originate from phylogenetically distant *Salmonella* provide
615 clues to understanding what drives promoter strength. Secondly, both homologous
616 and heterologous toxin/antitoxin systems can be used in *L. plantarum* for plasmid
617 retention without considerably affecting bacterial growth rates or protein production
618 levels. More interestingly, the plasmid retention efficacy of these systems can be
619 improved by combining two toxin-antitoxin systems, a phenomenon that has yet
620 been tested only in *E. coli*. Finally, these systems provide the possibility to generate
621 tunable transient GEMs since plasmid loss reverts the cells to their non-GEM
622 probiotic status, characterized by the new G_{50} metric.

623

624 **DATA AVAILABILITY**

625 All data are available from the corresponding authors upon reasonable request.

626 **SUPPLEMENTARY DATA**

627 Supplementary Data are available online.

628 **ACKNOWLEDGEMENT**

629 The *L. plantarum* WCFS1 strain was a kind gift from Prof. Gregor Fuhrmann
630 (Helmholtz Institute for Pharmaceutical Research, Saarland). The plasmids pSIP403
631 and pLp_3050sNuc were a kind gift from Prof. Lars Axelsson (Addgene plasmid #
632 122028) and Prof. Geir Mathiesen (Addgene plasmid # 122030) respectively. The
633 plasmid pTlpA39-Wasabi was a kind gift from Prof. Mikhail Shapiro (Addgene
634 plasmid # 86116). The plasmid pUC-GFP-AT was a kind gift from Prof. Chris Barnes
635 (Addgene plasmid # 133306). The authors thank Dr. Samuel Pearson at the INM –
636 Leibniz Institute for New Materials for discussions that led to the G₅₀ concept.

637 **FUNDING**

638 This work was supported by the Deutsche Forschungsgemeinschaft's Research grant
639 [Project # 455063657], Collaborative Research Centre, SFB 1027 [Project #
640 200049484] and the Leibniz Science Campus on Living Therapeutic Materials [LifeMat].

641 **CONFLICT OF INTEREST**

642 A patent application has been filed based on the results of this work (Application No.
643 is DE 10 2022 119 024.2).

644

645 **REFERENCES**

646 Abedi, M.H., Yao, M.S., Mittelstein, D.R., Bar-Zion, A., Swift, M.B., Lee-Gosselin, A., et
647 al. (2022) Ultrasound-controllable engineered bacteria for cancer immunotherapy. *Nat.*
648 *Commun.*, 13, 1-11.

649

650 Allison, G.E. and Klaenhammer, T.R. (1996) Functional analysis of the gene encoding
651 immunity to lactacin F, lafl, and its use as a *Lactobacillus*-specific, food-grade genetic
652 marker. *Appl. Environ. Microbiol.*, 62, 4450-4460.

653

654 Ashraf, R. and Shah, N.P. (2011) Selective and differential enumerations of
655 *Lactobacillus delbrueckii* subsp. *bulgaricus*, *Streptococcus thermophilus*, *Lactobacillus*
656 *acidophilus*, *Lactobacillus casei* and *Bifidobacterium* spp. in yoghurt--A review.
657 *Int. J. Food Microbiol.*, 149, 194-208.

658

659 Bardaji, L., Añorga, M., Echeverría, M., Ramos, C. and Murillo, J. (2019) The toxic
660 guardians—multiple toxin-antitoxin systems provide stability, avoid deletions and
661 maintain virulence genes of *Pseudomonas syringae* virulence plasmids. *Mobile*
662 *DNA.*, 10, 1-17.

663

664 Beaulaurier, J., Schadt, E.E. and Fang, G. (2019) Deciphering bacterial epigenomes
665 using modern sequencing technologies. *Nat. Rev. Genet.*, 20,157-172.

666

667 Bhusari, S., Sankaran, S. and Del Campo, A. (2022) Regulating bacterial behavior
668 within hydrogels of tunable viscoelasticity. *Adv. Sci.*, 9, p2106026.

669

670 Bibalan, M.H., Eshaghi, M., Rohani, M., Esghaei, M., Darban-Sarokhalil, D., Pourshafie,
671 M.R., et al. (2017) Isolates of *Lactobacillus plantarum* and *L. reuteri* display greater
672 antiproliferative and antipathogenic activity than other *Lactobacillus* isolates. *J. Med.*
673 *Microbiol.*, 66, 1416-1420.

674

675 Bron, P.A., Hoffer, S.M., Van Swam, I.I., De Vos, W.M. and Kleerebezem, M. (2004)
676 Selection and characterization of conditionally active promoters in *Lactobacillus*
677 *plantarum*, using alanine racemase as a promoter probe. *Appl. Environ. Microbiol.*, 70,
678 310-317.

679

- 680 Casadesús, J. and Low, D. (2006) Epigenetic gene regulation in the bacterial
681 world. *Microbiol. Mol. Biol. Rev.*, 70, 830-856.
- 682
- 683 Castillo-Hair, S.M., Baerman, E.A., Fujita, M., Igoshin, O.A. and Tabor, J.J. (2019)
684 Optogenetic control of *Bacillus subtilis* gene expression. *Nat. Commun.*, 10, 1-11.
- 685
- 686 Chan, M.Z.A., Chua, J.Y., Toh, M. and Liu, S.Q. (2019) Survival of probiotic strain
687 *Lactobacillus paracasei* L26 during co-fermentation with *S. cerevisiae* for the
688 development of a novel beer beverage. *Food Microbiol.*, 82, 541-550.
- 689 Chee, W.K.D., Yeoh, J.W., Dao, V.L. and Poh, C.L. (2022) Highly reversible tunable
690 thermal-repressible split-t7 RNA polymerases (thermal-T7RNAPs) for dynamic gene
691 regulation. *ACS Synthetic Biology*, 11(2), pp.921-937.
- 692 Chen, Y., Qi, M., Xu, M., Huan, H., Shao, W. and Yang, Y. (2018) Food-grade gene
693 transformation system constructed in *Lactobacillus plantarum* using a *GlmS*-encoding
694 selection marker. *FEMS Microbiol. Lett.*, 365, fny254.
- 695
- 696 Courbet, A., Endy, D., Renard, E., Molina, F. and Bonnet, J. (2015) Detection of
697 pathological biomarkers in human clinical samples via amplifying genetic switches and
698 logic gates. *Sci. Transl. Med.*, 7, 289ra83-289ra83.
- 699
- 700 Darby, T.M., and Jones, R.M. (2017) Beneficial influences of *Lactobacillus plantarum* on
701 human health and disease. In Floch, M., Ringel, Y., Walker, W.A. (ed.), *The microbiota*
702 *in gastrointestinal pathophysiology*. Academic Press, Vol. I, pp. 109-117.
- 703
- 704 Davis, M.C., Kesthely, C.A., Franklin, E.A. and MacLellan, S.R. (2017) The essential
705 activities of the bacterial sigma factor. *Can. J. Microbiol.*, 63, 89-99.
- 706
- 707 Dawoud, T.M., Davis, M.L., Park, S.H., Kim, S.A., Kwon, Y.M., Jarvis, N., O'Bryan, C.A.,
708 Shi, Z., Crandall, P.G. and Ricke, S.C. (2017) The potential link between thermal
709 resistance and virulence in *Salmonella*: a review. *Frontiers in veterinary science*, 4,
710 p.93.
- 711
- 712 de Vos, W.M. (2011) Systems solutions by lactic acid bacteria: from paradigms to
713 practice. *Microb. Cell Fact.*, 10, 1-13.

714

715 du Toit, M., Engelbrecht, L., Lerm, E. and Krieger-Weber, S. (2011) Lactobacillus: the
716 next generation of malolactic fermentation starter cultures—an overview.
717 Food Bioprocess Technol., 4, 876-906.

718

719 Edgar, R.C. (2004) MUSCLE: a multiple sequence alignment method with reduced time
720 and space complexity. BMC Bioinf., 5, 1-19.

721

722 Elowitz, M.B. and Leibler, S. (2000) A synthetic oscillatory network of transcriptional
723 regulators. Nature., 403, 335-338.

724

725 Fedorec, A.J., Ozdemir, T., Doshi, A., Ho, Y.K., Rosa, L., Rutter, J., et al. (2019) Two
726 new plasmid post-segregational killing mechanisms for the implementation of synthetic
727 gene networks in Escherichia coli. iscience., 14, 323-334.

728

729 Gaida, S.M., Sandoval, N.R., Nicolaou, S.A., Chen, Y., Venkataramanan, K.P. and
730 Papoutsakis, E.T. (2015) Expression of heterologous sigma factors enables functional
731 screening of metagenomic and heterologous genomic libraries. Nat. Commun., 6, 1-10.

732

733 Grady, R. and Hayes, F. (2003) Axe–Txe, a broad-spectrum proteic toxin–antitoxin
734 system specified by a multidrug-resistant, clinical isolate of Enterococcus
735 faecium. Mol. Microbiol., 47, 1419-1432.

736

737 Halbmayr, E., Mathiesen, G., Nguyen, T.H., Maischberger, T., Peterbauer, C.K., Eijsink,
738 V.G., et al. (2008) High-level expression of recombinant β -galactosidases in
739 Lactobacillus plantarum and Lactobacillus sakei using a sakacin P-based expression
740 system. J. Agric. Food Chem., 56, 4710-4719.

741

742 Heiss, S., Hörmann, A., Tauer, C., Sonnleitner, M., Egger, E., Grabherr, R. et al. (2016)
743 Evaluation of novel inducible promoter/repressor systems for recombinant protein
744 expression in Lactobacillus plantarum. Microb. Cell Factories., 15, 1-17.

745

- 746 Helmann, J.D. (1995) Compilation and analysis of *Bacillus Subtilis* σ A-dependent
747 promoter sequences: evidence for extended contact between RNA polymerase and
748 upstream promoter DNA. *Nucleic Acids Res.* 23, 2351-2360.
- 749
- 750 Hurme, R., Berndt, K.D., Normark, S.J. and Rhen, M. (1997) A proteinaceous gene
751 regulatory thermometer in *Salmonella*. *Cell.*, 90, 55-64.
- 752
- 753 Janahi, E.M.A., Haque, S., Akhter, N., Wahid, M., Jawed, A., Mandal, R.K., et al. (2018)
754 Bioengineered intravaginal isolate of *Lactobacillus plantarum* expresses algal lectin
755 scytovirin demonstrating anti-HIV-1 activity. *Microb. Pathog.*, 122, 1-6.
- 756
- 757 Jiménez, E., Fernández, L., Maldonado, A., Martín, R., Olivares, M., Xaus, J., et al.
758 (2008) Oral administration of *Lactobacillus* strains isolated from breast milk as an
759 alternative for the treatment of infectious mastitis during lactation. *Appl. Environ.*
760 *Microbiol.*, 74, 4650–4655
- 761
- 762 Kasımoğlu, A., Göncüoğlu, M. and Akgün, S. (2004) Probiotic white cheese with
763 *Lactobacillus acidophilus*. *Int. Dairy J.*, 14, 1067-1073.
- 764 Kan, A., Gelfat, I., Emani, S., Praveschotinunt, P. and Joshi, N.S. (2020) Plasmid
765 vectors for in vivo selection-free use with the probiotic *E. coli* Nissle 1917. *ACS*
766 *synthetic biology*, 10(1), pp.94-106.
- 767
- 768 Landete, J.M., Langa, S., Revilla, C., Margolles, A., Medina, M. and Arqués, J.L. (2015)
769 Use of anaerobic green fluorescent protein versus green fluorescent protein as reporter
770 in lactic acid bacteria. *Appl. Microbiol. Biotechnol.*, 99, 6865-6877.
- 771
- 772 LeCureux, J.S. and Dean, G.A. (2018) *Lactobacillus* mucosal vaccine vectors: immune
773 responses against bacterial and viral antigens. *mSphere.*, 3, e00061-18.
- 774
- 775 Letunic, I. and Bork, P. (2007) Interactive Tree Of Life (iTOL): an online tool for
776 phylogenetic tree display and annotation. *Bioinformatics.*, 23, 127-128.

- 777 Levante, A., Folli, C., Montanini, B., Ferrari, A., Neviani, E. and Lazzi, C. (2019)
778 Expression of DinJ-YafQ System of *Lactobacillus casei* group strains in response to
779 food processing stresses. *Microorganisms.*, 7, 438.
- 780
- 781 Ma, B., Forney, L.J. and Ravel, J. (2012) The vaginal microbiome: rethinking health and
782 diseases. *Annu. Rev. Microbiol.*, 66, 371.
- 783
- 784 Mastromarino, P., Macchia, S., Meggiorini, L., Trinchieri, V., Mosca, L., Perluigi, M., et
785 al. (2009) Effectiveness of *Lactobacillus*-containing vaginal tablets in the treatment of
786 symptomatic bacterial vaginosis. *Clin. Microbiol. Infect.*, 15, 67-74.
- 787
- 788 Mathiesen, G., Øverland, L., Kuczkowska, K. and Eijsink, V.G. (2020) Anchoring of
789 heterologous proteins in multiple *Lactobacillus* species using anchors derived from
790 *Lactobacillus plantarum*. *Sci. Rep.*, 10, 1-10.
- 791
- 792 Mathiesen, G., Sveen, A., Brurberg, M.B., Fredriksen, L., Axelsson, L. and Eijsink, V.G.
793 (2009) Genome-wide analysis of signal peptide functionality in *Lactobacillus plantarum*
794 WCFS1. *BMC genomics.*, 10, 1-13.
- 795
- 796 Madeira, F., Pearce, M., Tivey, A., Basutkar, P., Lee, J., Edbali, O., et al. (2022) Search
797 and sequence analysis tools services from EMBL-EBI in 2022. *Nucleic Acids Res.*
- 798
- 799 Meier-Kolthoff, J.P. and Göker, M. (2019) TYGS is an automated high-throughput
800 platform for state-of-the-art genome-based taxonomy. *Nat. Commun.*, 10, 1-10.
- 801
- 802 Meng, Q., Yuan, Y., Li, Y., Wu, S., Shi, K. and Liu, S. (2021) Optimization of
803 electrotransformation parameters and engineered promoters for *Lactobacillus plantarum*
804 from wine. *ACS Synth. Biol.*, 10, 1728-1738.
- 805
- 806 Nguyen, T.T., Mathiesen, G., Fredriksen, L., Kittl, R., Nguyen, T.H., Eijsink, V.G., et al.
807 (2011) A food-grade system for inducible gene expression in *Lactobacillus plantarum*

808 using an alanine racemase-encoding selection marker. *J. Agric. Food Chem.*, 59, 5617-
809 5624.

810

811 Nguyen, H.M., Pham, M.L., Stelzer, E.M., Plattner, E., Grabherr, R., Mathiesen, G.,
812 Peterbauer, C.K., Haltrich, D. and Nguyen, T.H. (2019) Constitutive expression and cell-
813 surface display of a bacterial β -mannanase in *Lactobacillus plantarum* *Microb. Cell*
814 *Factories*, 18,1-12.

815

816

817 Paget, M.S. and Helmann, J.D. (2003) The σ 70 family of sigma factors. *Genome Biol.*, 4,
818 1-6.

819

820 Pedrolli, D.B., Ribeiro, N.V., Squizzato, P.N., de Jesus, V.N., Cozetto, D.A., Tuma, R.B.,
821 et al. (2019) Engineering microbial living therapeutics: the synthetic biology
822 toolbox. *Trends Biotechnol.*, 37, 100-115.

823

824 Piraner, D.I., Abedi, M.H., Moser, B.A., Lee-Gosselin, A. and Shapiro, M.G. (2017)
825 Tunable thermal bioswitches for in vivo control of microbial therapeutics. *Nat. Chem.*
826 *Biol.*, 13, 75-80.

827

828 Plessas, S., Fisher, A., Koureta, K., Psarianos, C., Nigam, P. and Koutinas, A.A. (2008)
829 Application of *Kluyveromyces marxianus*, *Lactobacillus delbrueckii* ssp. *bulgaricus* and
830 *L. helveticus* for sourdough bread making. *Food Chem.*, 106, 985-990.

831

832 Rosenfeldt, V., Benfeldt, E., Nielsen, S.D., Michaelsen, K.F., Jeppesen, D.L., Valerius,
833 N.H., et al. (2003) Effect of probiotic *Lactobacillus* strains in children with atopic
834 dermatitis. *J. Allergy Clin. Immunol.*, 111, 389-395.

835 Rottinghaus, A.G., Ferreira, A., Fishbein, S.R., Dantas, G. and Moon, T.S. (2022)
836 Genetically stable CRISPR-based kill switches for engineered microbes. *Nature*
837 *communications*, 13(1), pp.1-17.

838

839 Rud, I., Jensen, P.R., Naterstad, K. and Axelsson, L. (2006) A synthetic promoter library
840 for constitutive gene expression in *Lactobacillus plantarum*. *Microbiology.*, 152, 1011-
841 1019.

842

- 843 Russo, P., Iturria, I., Mohedano, M.L., Caggianiello, G., Rainieri, S., Fiocco, D., et al.
844 (2015) Zebrafish gut colonization by mCherry-labelled lactic acid bacteria. *Appl.*
845 *Microbiol. Biotechnol.*, 99, 3479-3490.
- 846
- 847 Salomé-Desnoulez, S., Poiret, S., Foligné, B., Muharram, G., Peucelle, V., Lafont, F., et
848 al. (2021) Persistence and dynamics of fluorescent *Lactobacillus plantarum* in the
849 healthy versus inflamed gut. *Gut Microbes.*, 13, 1897374.
- 850
- 851 Siezen, R.J. and van Hylckama Vlieg, J.E. (2011) Genomic diversity and versatility of
852 *Lactobacillus plantarum*, a natural metabolic engineer. *Microb. Cell Factories.*, 10, 1-13.
- 853
- 854 Stirling, F. and Silver, P.A. (2020) Controlling the implementation of transgenic microbes:
855 are we ready for what synthetic biology has to offer? *Molecular cell*, 78(4), pp.614-623.
- 856
- 857 Sørvig, E., Grönqvist, S., Naterstad, K., Mathiesen, G., Eijsink, V.G. and Axelsson, L.
858 (2003) Construction of vectors for inducible gene expression in *Lactobacillus sakei* and
859 *L. plantarum*. *FEMS Microbiol. Lett.*, 229, 119-126.
- 860
- 861 Sørvig, E., Mathiesen, G., Naterstad, K., Eijsink, V.G. and Axelsson, L. (2005a) High-
862 level, inducible gene expression in *Lactobacillus sakei* and *Lactobacillus plantarum*
863 using versatile expression vectors. *Microbiology.*, 151, 2439-2449.
- 864 Sørvig, E., Skaugen, M., Naterstad, K., Eijsink, V.G. and Axelsson, L. (2005b) Plasmid
865 p256 from *Lactobacillus plantarum* represents a new type of replicon in lactic acid
866 bacteria, and contains a toxin-antitoxin-like plasmid maintenance system. *Microbiology*,
867 151, 421-431.
- 868
- 869
- 870 Spangler, J.R., Caruana, J.C., Phillips, D.A. and Walper, S.A. (2019) Broad range
871 shuttle vector construction and promoter evaluation for the use of *Lactobacillus*
872 *plantarum* WCFS1 as a microbial engineering platform. *Synth. Biol.*, 4, ysz012.
- 873 Spath, K., Heinl, S. and Grabherr, R. (2012) Direct cloning in *Lactobacillus plantarum*:
874 electroporation with non-methylated plasmid DNA enhances transformation efficiency
875 and makes shuttle vectors obsolete. *Microb. Cell Factories.*, 11, 1-8.

876

877 Takala, T. and Saris, P. (2002) A food-grade cloning vector for lactic acid bacteria
878 based on the nisin immunity gene nisl. *Appl. Microbiol. Biotechnol.*, 59, 467-471.

879

880 Tauer, C., Heintl, S., Egger, E., Heiss, S. and Grabherr, R. (2014) Tuning constitutive
881 recombinant gene expression in *Lactobacillus plantarum*. *Microb. Cell Factories.*, 13, 1-
882 11.

883

884 Teughels, W., Durukan, A., Ozcelik, O., Pauwels, M., Quirynen, M. and Haytac, M.C.
885 (2013) Clinical and microbiological effects of *Lactobacillus reuteri* probiotics in the
886 treatment of chronic periodontitis: a randomized placebo-controlled study. *J. Clin.*
887 *Periodontol.*, 40, 1025-1035.

888

889 Todt, T.J., Wels, M., Bongers, R.S., Siezen, R.S., Van Hijum, S.A. and Kleerebezem, M.
890 (2012) Genome-wide prediction and validation of sigma70 promoters in *Lactobacillus*
891 *plantarum* WCFS1. *PLoS One.*, 7, e45097

892

893 Tran, A.M., Unban, K., Kanpiengjai, A., Khanongnuch, C., Mathiesen, G., Haltrich, D.
894 and Nguyen, T.H. (2021) Efficient secretion and recombinant production of a
895 lactobacillal α -amylase in *Lactiplantibacillus plantarum* WCFS1: analysis and
896 comparison of the secretion using different signal peptides. *Front. Microbiol.*, 12,
897 689413.

898

899

900 Turrone, F., Ventura, M., Buttó, L.F., Duranti, S., O'Toole, P.W., Motherway, M.O.C., et
901 al. (2014) Molecular dialogue between the human gut microbiota and the host: a
902 *Lactobacillus* and *Bifidobacterium* perspective. *Cell. Mol. Life Sci.*, 71,183-203.

903

904 Van Kranenburg, R., Golic, N., Bongers, R., Leer, R.J., De Vos, W.M., Siezen, R.J., et
905 al. (2005) Functional analysis of three plasmids from *Lactobacillus plantarum*. *Appl.*
906 *Environ. Microbiol.*, 71, 1223-1230.

907

908 Wang, M., Fu, T., Hao, J., Li, L., Tian, M., Jin, N., et al. (2020) A recombinant
909 *Lactobacillus plantarum* strain expressing the spike protein of SARS-CoV-2. *Int. J. Biol.*
910 *Macromol.*, 160, 736-740.

911
912 Wang, B., Kitney, R.I., Joly, N. and Buck, M. (2011) Engineering modular and
913 orthogonal genetic logic gates for robust digital-like synthetic biology. *Nat. Commun.*, 2,
914 1-9.

915
916 Waterhouse, A.M., Procter, J.B., Martin, D.M., Clamp, M. and Barton, G.J. (2009)
917 Jalview Version 2—a multiple sequence alignment editor and analysis
918 workbench. *Bioinformatics.*, 25, 1189-1191.

919
920 Watterlot, L., Rochat, T., Sokol, H., Cherbuy, C., Bouloufa, I., Lefèvre, F., et al. (2010)
921 Intragastric administration of a superoxide dismutase-producing recombinant
922 *Lactobacillus casei* BL23 strain attenuates DSS colitis in mice.
923 *Int. J. Food Microbiol.*, 144, 35-41.

924
925 Wright, O., Stan, G.B. and Ellis, T.(2013) Building-in biosafety for synthetic biology.
926 *Microbiology*, 159(Pt_7), pp.1221-1235.

927 Xie, Y., Wei, Y., Shen, Y., Li, X., Zhou, H., Tai, C et al. (2018) TADB 2.0: an updated
928 database of bacterial type II toxin–antitoxin loci. *Nucleic Acids Res.*, 46, D749-D753.

929
930 Yamaguchi, Y. and Inouye, M. (2011) Regulation of growth and death in *Escherichia*
931 *coli* by toxin–antitoxin systems. *Nat. Rev. Microbiol.*, 9, 779-790.

932
933 Zheng, J., Wittouck, S., Salvetti, E., Franz, C.M., Harris, H.M., Mattarelli, P., et al.
934 (2020) A taxonomic note on the genus *Lactobacillus*: Description of 23 novel genera,
935 emended description of the genus *Lactobacillus* Beijerinck 1901, and union of
936 *Lactobacillaceae* and *Leuconostocaceae*. *Int. J. Syst. Evol. Microbiol.*, 70, 2782-2858.

937
938 Zocco, M. A., Verme L. Z.D., Cremonini, F., Piscaglia, A.C., Nista, E.C., Candelli, M., et
939 al. (2006) Efficacy of *Lactobacillus* GG in maintaining remission of ulcerative
940 colitis. *Aliment. Pharmacol. Ther.*, 23, 1567-1574.

941

942

943

944 **FIGURE LEGENDS**

945 **Figure 1.** (A) Phylogenetic tree highlighting the distances between species from
946 which various genetic parts have been tested in *L. plantarum*. Purple clade
947 corresponds to Gram-negative bacteria. Green clade corresponds to Gram-positive
948 bacteria. Promoters tested in this study are labelled in blue. Promoters tested by
949 others in *L. plantarum* are labelled in green. Orange labels correspond to the TA
950 systems tested in this study. (B) Fluorescence microscopy of P_{tIpA} driven mCherry
951 expression in *L. plantarum* WCFS1 cultivated at 31°C and 39°C for 18 h. Scale bar
952 = 10 μ m (C) Flow Cytometry analysis of P_{tIpA} , P_{23} , P_{48} , P_{spp} and P_{Tuf} driven mCherry
953 expression in *L. plantarum* WCFS1 after 18 h incubation at 37°C. (D) Fluorescence
954 spectroscopy analysis of the P_{tIpA} , P_{23} , P_{48} , P_{spp} and P_{Tuf} driven mCherry expression
955 after 18 h incubation at temperatures ranging from 31°C to 41°C. (E) Growth rate
956 (OD_{600}) measurement of *L. plantarum* WCFS1 strains containing a control plasmid
957 and P_{tIpA} -mCherry for 18 h at 37°C. In (C) and (D), the solid lines represent mean
958 values, and the lighter bands represents standard deviations calculated from three
959 independent biological replicates.

960

961 **Figure 2.** (A) Homology analysis of $\sigma 70$ RpoD genes from *L. plantarum*, *E. coli*, and
962 *S. typhimurium*. Height and brightness of the yellow bars indicate the extent to
963 which individual residues are conserved across all 3 bacteria. (B) P_{tIpA} promoter
964 sequence with -35, spacer and -10 regions labelled

965

966 **Figure 3.** (A) Schematic Representation of cloning the different TA genetic modules into
967 the P_{tIpA} -mCherry plasmid. (B) Sample flow Cytometry histogram plot of the P_{tIpA} -
968 mCherry plasmid containing strain without any TA module or selection pressure after 50
969 generations of serial passaging in the absence of antibiotic. The green box corresponds
970 to the bacterial population retaining the plasmid and the blue box represents the
971 population devoid of the plasmid. (C) Plasmid retention analysis of the TA module
972 containing strains for 100 generations without antibiotics along with no TA and antibiotic
973 selection pressure conditions for comparison. (D) Growth rate (OD_{600}) of strains with the
974 TA modules, no TA and antibiotic retention over 10 generations at 37°C. In (C) and (D),
975 the solid lines represent mean values and the lighter bands represents SD calculated
976 from three independent biological replicates. Combo = MazF/MazE + YafQ/DinJ . (E)

977 Flow cytometry plots of strains containing TA modules, no TA and antibiotic retention
978 after 10 generations. The Y-axis for each plot represents counts with plot heights in the
979 range of 450 – 500 (F) Fluorescence Spectroscopy analysis of strains containing TA
980 modules, no TA and antibiotic retention after 10 generations. The relative intensity has
981 been plotted for all the TA strains by normalizing their respective fluorescence values
982 against the “No TA” strain. The data represents three independent biological replicates.
983 p-values are calculated using one-way ANOVA with Tukey test on respective means (*
984 $p < 0.05$, *** $p < 0.001$). The “No TA”, “Txe-Axe” and “Antibiotic” conditions are significantly
985 different from other candidates, so their p - values have not been explicitly highlighted.

986

987 **Figure 4.** G_{50} values of the different TA systems tested in *L. plantarum*. Combo =
988 MazF/MazE + YafQ/DinJ

989